Journal of Power Sources 215 (2012) 301–306

Contents lists available at SciVerse ScienceDirect

Journal of Power Sources

journal homepage: www.elsevier.com/locate/jpowsour

Porous YSZ impregnated with $La_{0.4}Sr_{0.5}Ba_{0.1}TiO_3$ as a possible composite anode for SOFCs fueled with sour feeds

Adrien L. Vincent [a], Amir R. Hanifi [a], Jing-Li Luo [a,*], Karl T. Chuang [a], Alan R. Sanger [a], Thomas H. Etsell [a], Partha Sarkar [b]

[a] Department of Chemical and Materials Engineering, University of Alberta, Edmonton, Alberta, Canada T6G 2G6
[b] Environment & Carbon Management Division, Alberta Innovates – Technology Futures, Edmonton, Alberta, Canada T6N 1E4

HIGHLIGHTS

- The catalytic activity of the anodes increased with the amount of LSBT up to an optimum value.
- H_2S promotes the hydrogen and the methane activation on LSBT.
- Impregnation is a better choice for anode preparations than powder mixtures.
- The fuel mixture Methane H_2S, can provides a very high power density compared to respective single gases.
- The impregnation process allows construction of anode supported SOFC membranes.

ARTICLE INFO

Article history:
Received 24 February 2012
Received in revised form
19 April 2012
Accepted 20 April 2012
Available online 18 May 2012

Keywords:
SOFC
Porous YSZ
Microstructure
$La_{0.4}Sr_{0.5}Ba_{0.1}TiO_3$
Impregnation
Perovskite

ABSTRACT

The system LSBT/YSZ (LSBT is $La_{0.4}Sr_{0.5}Ba_{0.1}TiO_3$) is a promising combination as an anode material for full ceramic SOFCs. An anode comprising a porous layer of YSZ impregnated with LSBT shows good performance for conversion of high sulfur content fuels. The microstructures within the composite matrix were determined and correlated with the parameters of the production process. The anodes were characterized electrochemically using impedance spectroscopy (EIS) and potentiodynamic tests performed at 850 °C with various fuels to determine the effect of H_2S in the feeds: H_2, H_2/H_2S (5000 ppm), CH_4, CH_4/H_2S (5000 ppm). The highest power densities (200 mW cm^{-2} in H_2/H_2S) were obtained for LSBT/YSZ composites after impregnation six times with LSBT, corresponding to 12.6 wt% LSBT; further impregnations dramatically decreased performance as a result of restricted access of fuel to active sites.

1. Introduction

A major source of interest in solid oxide fuel cells (SOFCs) arises from their theoretical capability to use any oxidizable feed as fuel. Unfortunately, several prospective catalyst materials presently used in anodes are readily poisoned by one or more possible impurities in anode feed gases [1–3]. Hence, the current generation of commercial SOFCs typically operates on pure hydrogen, an expensive feed, to ensure both good performance and good stability [4,5].

The majority of industrial H_2 is manufactured by conversion of hydrocarbon resources, for example, by steam reforming. Major anode catalyst poisons present in fuels derived from coal or lighter hydrocarbons are CO and H_2S. While it is possible to oxidize H_2S as a fuel [6,7], the most efficient H_2 SOFC catalysts, notably Pt, Pd and the cermet Ni-YSZ, react rapidly with H_2S either to form a sulfide or to poison the catalyst surface, even at low concentrations [8]. Therefore, one of the main challenges in development of new SOFCs is to enhance the stability of the anode in the presence of H_2S.

Recently, it was shown that lanthanum strontium titanate [9–12] (LST, $La_xSr_yTiO_3$) is a promising anode material. In H_2–air fuel cells the performance of LST anodes was shown to be comparable (in its initial state) with that obtained from the widely used cermet Ni/YSZ [13]. Additionally, LST appeared to be stable under a reducing environment containing H_2S [14] and the presence of

* Corresponding author. Tel.: +1 780 492 2232.
E-mail address: jingli.luo@ualberta.ca (J.-L. Luo).

0378-7753/$ – see front matter © 2012 Elsevier B.V. All rights reserved.
doi:10.1016/j.jpowsour.2012.04.063

H_2S even improved performance [15]. The interest in LSBT development is arising mainly from this ability as Ni/YSZ can only accept 10th of ppm of H_2S.

Impregnation of fuel cell electrodes with electrochemically active additives can improve their performance through enhancing one or both of the ionic or electronic pathways and the catalytic activity. Impregnation with nano-sized dispersed particles can serve two beneficial functions by enhancing the catalytic activity while the interconnected particles also may serve as the conduction paths. These advances in development of high performance electrode microstructures are a consequence of lower heat treatment temperatures when compared with the high temperature sintering used for the conventional electrodes [16,17].

We now will describe development of new anode catalysts comprising porous YSZ into which LSBT is impregnated. Different processes were tested for fabricating a porous YSZ matrix for subsequent impregnation with an LSBT precursor solution. The performance of LSBT/YSZ as an anode is correlated with its method of manufacture.

2. Experimental procedure

To prepare the porous YSZ layer, 8 mol% Y_2O_3 (YSZ, Tosoh) was calcined at 1500 °C for 3 h, mixed with water and ball milled using 5 mm ZrO_2 balls at 120 rpm for 72 h. The ratio of ZrO_2 balls to YSZ powder was set at 6:1 to provide a sufficient load to crush the coarse powders. The resultant fine YSZ powders had larger particle size (750 nm) and lower surface area (3.23 $m^2\ g^{-1}$) when compared with commercially available powder (Tosoh; particle size: 250 nm, surface area: 13.19 $m^2\ g^{-1}$). To achieve a high level of porosity in the anode layer 20 vol.% graphite (<325 mesh, Sigma Aldrich) or polymer microspheres (polymethylmethacrylate PMMA Spheromers, CA 6, Microbeads, Skedsmokorset, Norway), were mixed with glycerin to generate about 55 vol.% porosity after sintering at 1350 °C.

Using the ground and calcined powder, a much lower amount of pore former (20%) produced the required porosity and pore structure. These observations were consistent with previous reports showing the importance of YSZ calcination on fabrication of porous supports [18,19].

$La_{0.4}Sr_{0.5}Ba_{0.1}TiO_3$ (LSBT) precursor solution was prepared (Fig. 1) for impregnation from lanthanum nitrate $La(NO_3)_3.6H_2O$ (Alfa Aesar 99.9%), strontium nitrate $Sr(NO_3)_2$ (Sigma Aldrich), barium nitrate $Ba(NO_3)_2$ (Alfa Aesar 99+%) and titanium isopropoxide (TIP; Sigma Aldrich). The starting nitrate materials were first mixed in ultra pure water to form a solution having a total cation concentration of 1×10^{-3} mol g^{-1}. TIP was stabilized in triethanolamine (TEA; Sigma Aldrich; molar ratio TIP/TEA = 1/4) to which citric acid (CA; Alfa Aesar 99.5%) was added (molar ratio TIP/CA = 1/4). The vigorously stirred salt solution was added slowly to the TIP–TEA–CA mixture, and ultra pure water was added to provide a solution equivalent to an LSBT concentration of 128 g L^{-1}. The solution was evaporated, and the residue was dried and calcined to yield LSBT, about 2.2% of the original volume of the solution. Data related to LSBT have been previously published [15,20].

Fuel cells were fabricated using commercial YSZ disks (Fuelcellmaterials) as electrolyte, 300 μm thick and 25 mm in diameter, which also served as the cell support. The anode layer was prepared from an intimate mixture of the YSZ powders and a pore former dispersed in glycerin. The ink was deposited using tape casting and the combination was sintered to form assemblies with circular 1 cm^2 anodes.

The anode layers of sintered membranes were impregnated under vacuum with the LSBT precursor solution and heat treated at 800 °C for 1 h in air between successive impregnation steps to ensure good distribution of the catalyst phase. After the final anode catalyst impregnation and calcination in each sequence, the composite cathode (YSZ/LSM 50/50 wt%) was applied using tape casting and the assemblies were calcined at 1200 °C for 1 h in air. After calcination and cooling to room temperature, gold was applied as paste onto the anode side and platinum paste onto the cathode side; then both pastes were then pre-dried at 130 °C and sintered in-situ to form current collectors.

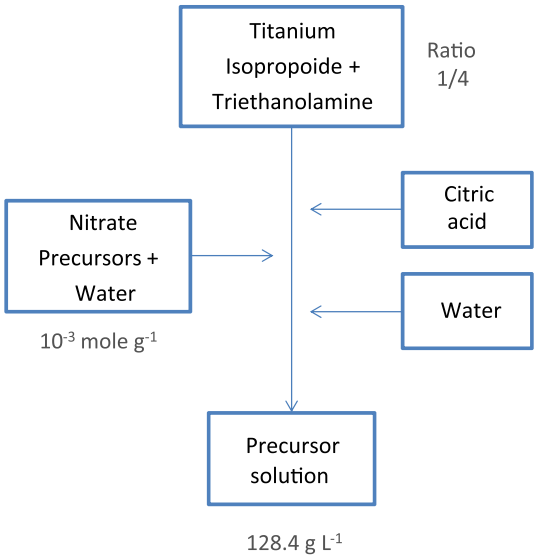

Fig. 1. Schematic of precursor solution preparation.

Single cell electrochemical testing was performed in a vertical furnace using a coaxial two-tube (inlet and outlet) set-up, as described elsewhere [20]. The outer tube (outlet) was sealed (Ceramabond, Aremco Products) directly to the outer edge of the anode side of the single cell electrolyte. Anodes were reduced in-situ before testing. The cathode side of each membrane electrode assembly (MEA) was not sealed to a tube, and was open to air.

The fuels used were pure methane (CH_4), methane with 0.5% hydrogen sulfide (CH_4/H_2S), pure hydrogen (H_2), and hydrogen with 0.5% hydrogen sulfide (H_2/H_2S); each was fed dry at the same flow rate (50 mL min^{-1}) to enable direct comparisons. In each sequence of anode tests, fuels were supplied sequentially in the following order: $H_2 \rightarrow CH_4 \rightarrow H_2/H_2S \rightarrow CH_4/H_2S$. This sequence was used as it was found that it required the minimum time for stabilization of electrochemical performance following each change of the feed. There were no irreversible adverse effects on the performance of the fuel cell arising from use of each fuel, and each of the observed phenomena was repeatable.

Electrochemical properties were reported without compensation for potentiodynamic analysis at 10 mV s^{-1} using a Solartron instrument (SI 1287).

The cross-sectional microstructures of the used MEA after use were observed using scanning electron microscopy (Hitachi S-2700) on fractured membranes.

3. Results and discussion

3.1. Impregnation of LSBT into porous YSZ

To study the impregnation process we compared two different kinds of porous matrix. Tests were performed on matrices comprised of porous YSZ fragments from fabricated tubes. Two different pore formers were used to prepare the YSZ matrices and

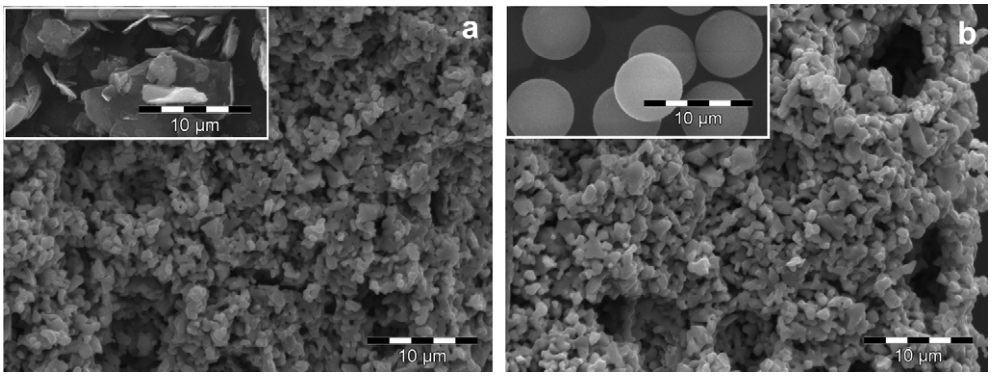

Fig. 2. SEM images of anode matrix produced using different pore formers: a) graphite; b) PMMA, with inserts of their respective pore former.

each produced matrices with about 55% porosity. Fig. 2 shows SEM images of the anode matrices prior to impregnation. The same precursor solution was used for all impregnations. Fig. 3 shows the mass gain for the two porous supports as a function of the number of times LSBT was impregnated. In both cases the mass gains were close to linear for up to 10 impregnation steps. The average mass gain was 2.1% per impregnation for porous YSZ when using PMMA as pore former (77% of the maximum impregnation) and 2.4% per impregnation when using graphite (93% of the maximum impregnation). Thus graphite appears to be the better pore former as it allows a significantly higher level of impregnation than PMMA. While the reason for the difference is not discernable from the present data, the microstructure obtained using PMMA as pore former showed some large pores. Consequently, it is conjectured that there was insufficient capillary force to maintain the solution within those larger pores.

When graphite was used as pore former the matrix showed some long, narrow pores, the shapes of which were similar to those of graphite "flakes", and these more easily retained the precursor solution. However, the pores obtained using graphite were oriented in parallel with the electrolyte, which was undesirable for good gas diffusion throughout the matrix, and which may have been a cause for performance instability, as described below.

PMMA was selected as the preferred pore former as it formed porous YSZ layers having an isotropic matrix which did not cause the instability in performance that occurred when using the YSZ matrix formed with graphite as pore former.

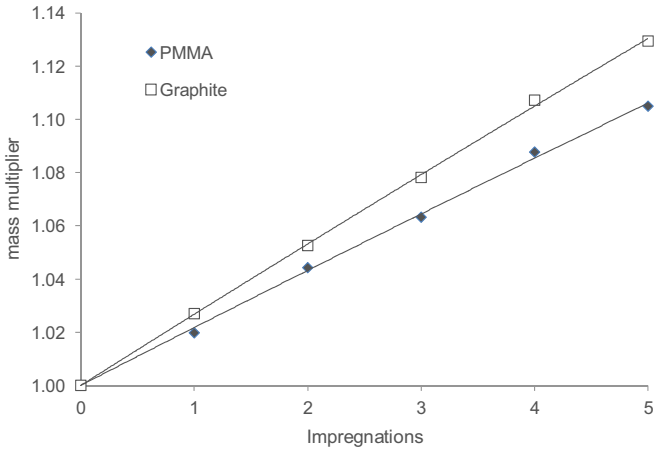

Fig. 3. Matrix mass gain as a function of the amount of impregnation and type of pore former.

SEM images showing microstructures of YSZ matrices prepared from PMMA and having different numbers of impregnations with LSBT are compared in Fig. 4. When there was only one impregnation the added LSBT was not evident due to the small amount, and LSBT grains were hard to differentiate from those of YSZ. As the number of impregnation steps increased the LSBT did not appear as an obvious, discrete phase; however, its presence was obvious from the visible reduction in porosity.

The SEM data showed LSBT blocking access to some clusters of pores without necessarily filling the pores themselves. As a result, a small amount of LSBT was sufficient to block a significant portion of the volume of active material. This phenomenon is attributable to the impregnation process itself. As the precursor solution dried in the matrix, the gel became concentrated by capillarity to the narrower zones between grains that were close to each other. With an increasing number of impregnation steps, the LSBT slowly formed deposits that closed the spaces between grains, and finally blocked an entire zone without filling the pores therein. Consequently, based on these SEM observations, it is inappropriate to deposit large amounts of LSBT through a large number of impregnations, as this will only serve to reduce the accessible volume of active material instead of increasing the number of active sites.

3.2. Cell performance

3.2.1. Impedance studies

To understand the effect of impregnation on the cell activity, we first determined the effect of impregnation of LSBT on impedance. Fig. 5 compares the impedance data of a cell without LSBT impregnated with those with up to ten impregnation steps. The top of Fig. 5 shows the Nyquist curve obtained after the sixth impregnation at 850 °C in H_2/H_2S as an example to highlight the meaning of the measured resistances of the other curves (not included). A pure ohmic resistance and two different semi-circles can be assigned in our system as high, medium and low frequency phenomena. Considering R1 called "resistance" or "ohmic polarization", the data show that after the second impregnation the loss already dropped by a factor of 4 to an apparently stable value. The ohmic loss considers all the cell components including the thick electrolyte, the anode thickness remains thin but un-impregnated its high porosity provides a major ohmic loss compared with the electrolyte. The addition of an electronic conductor like LSBT even a in small amount (two impregnations) is enough to significantly reduce the ohmic loss in the anode and to minimize it compared with the electrolyte. The dominant electrolyte resistance explains why R1 is not very sensitive to the amount of impregnation.

Determining the phenomenon related to R2 is more delicate. Assumed to be the charge transfer or activation polarization, this

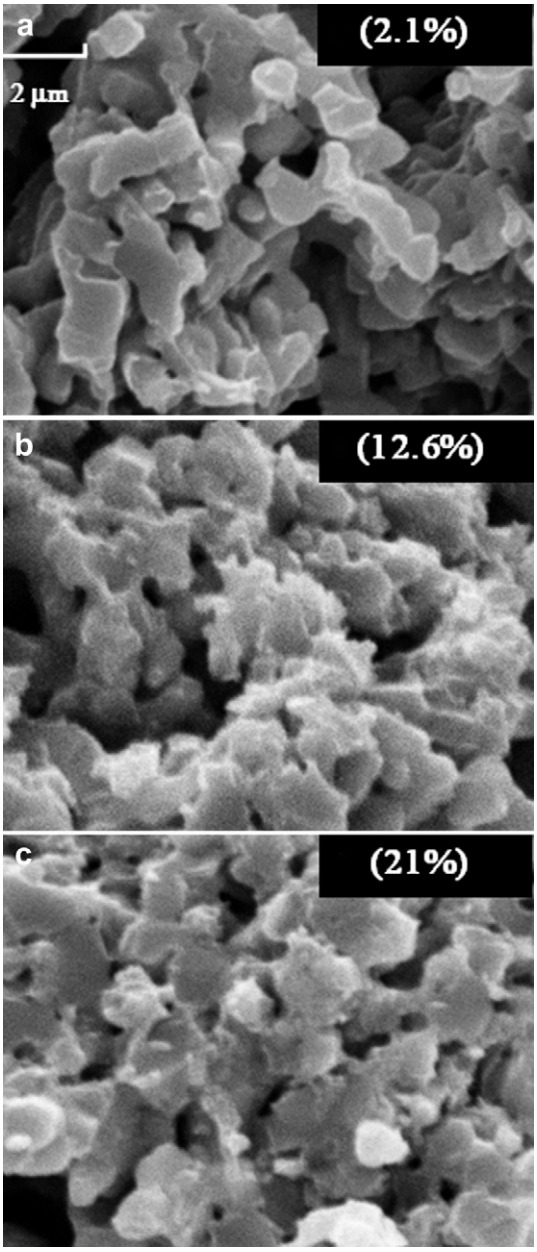

Fig. 4. Anode microstructure as a function of number of impregnations of LSBT into YSZ: a) 1 time, b) 6 times, and c) 10 times. The given percentage shows the LSBT mass gained.

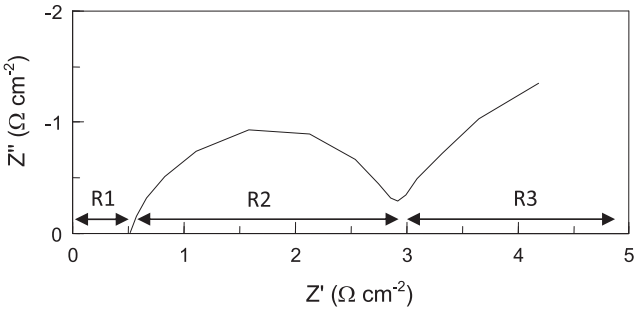

X=	0	2	4	6	8	10
			H2			
R1	2.30	0.68	0.55	0.62	0.58	0.63
R2	4.9	2.9	2.9	3.0	3.7	6.2
R3	138	70.0	58.5	35.7	35.7	23.9
			CH4			
R1	2.30	0.75	0.60	0.58	0.53	0.56
R2	4.2	3.5	2.8	2.7	3.3	6.1
R3	10000	1400	250	73.0	49.7	16.5
			H2/H2S			
R1	2.30	0.69	0.53	0.64	0.60	0.68
R2	3.7	2.2	2.2	2.5	2.9	6.1
R3	120	30.0	14.2	9.2	7.8	13.9
			CH4/H2S			
R1	2.30	0.70	0.55	0.57	0.54	0.62
R2	3.8	2.0	1.9	2.3	3.1	6.3
R3	122	50.9	8.4	4.7	4.6	4.1

Fig. 5. Impedances data (ohm) for LSBT/YSZ anodes at 850 °C for different feed gases as a function of number of times (×) LSBT was impregnated.

phenomenon is critical in its effect on the overall cell performance. As a result, cell performance follows exactly the same trend as R2. Increasing the thickness of LSBT doesn't change its activity with the fuels which explains the relative stability of R2 between the second and the eighth impregnation. The data in Fig. 5 also show that the addition of H_2S has a very important effect on the charge transfer phenomenon. We explained in our previous work [15] that sulfur interacts with the surface layers of LSBT and becomes a rapidly exchanged charged element. After the eighth impregnation, R2 increases dramatically and reaches a similar value for all the gases ($\sim$6.1 Ω cm^{-2}). This means that the fuel activity and "selectivity" becomes very poor. When the amount of LSBT was increased the triple phase boundary (TPB) also increased until there was an excess of LSBT (Eighth impregnation) and access to the surface became obstructed.

R3 (related to a low frequency phenomenon) ascribed to diffusion or concentration polarization decreases linearly with the number of impregnations for pure H_2 and pure CH_4. In the case of poisoned gases, R3 stabilizes at a low value from the sixth impregnation. This observed stabilization is related to the high H_2S coverage on LSBT. The exact origin for this stable state is not evident; H_2S itself could be a limiting factor in the diffusion process also, a complex chemistry (about the real adsorbed species) between the main fuel and H_2S could be at the origin of this stabilization and could be a reason for the differences between H_2/H_2S and CH_4/H_2S.

These impedance studies indicated that the anode having porous YSZ impregnated six times with LSBT has the best combination of low ohmic, charge transfer and polarization resistances.

3.2.2. Fuel cell performance

I/V curves provide more insight than a single maximum power value. Fig. 6 shows the I/V curves obtained at 850 °C for the four different feed gases using a membrane assembly having an anode with six LSBT impregnations.

Fig. 6a (dashed) was obtained using pure CH_4 as feed. As expected, the maximum current density was low but the maximum power density was in the same range as H_2. The curve shapes had two distinctive parts: a high voltage domain, where the I/V curve showed reasonable performance and a low voltage domain where there was a sudden, strong decrease in current density. Comparison with the I/V curve obtained with sour gas (Fig. 6b) is interesting as the shape looks similar with more abrupt changes. This behavior

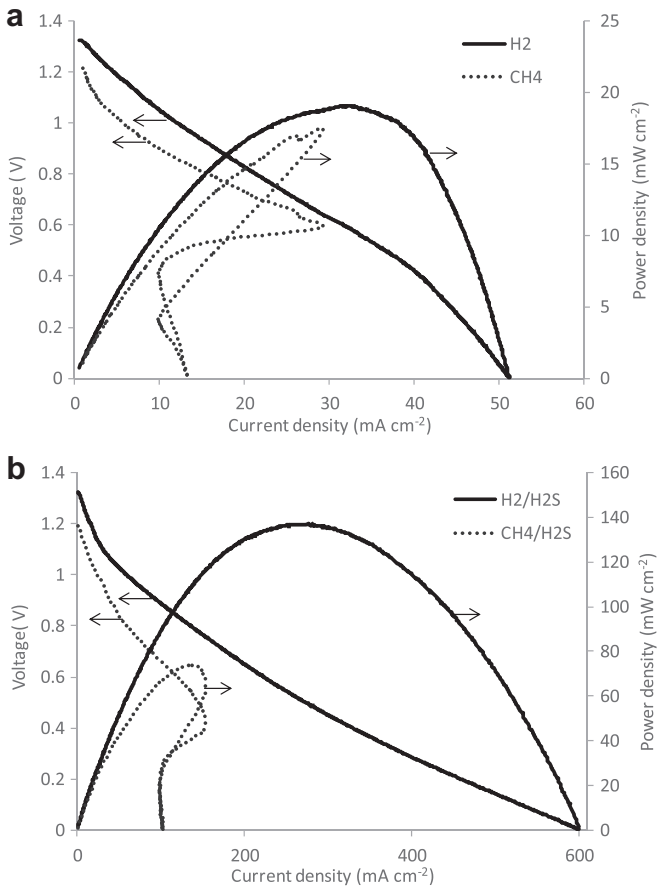

Fig. 6. Uncompensated I/V curves and power density curves obtained at 850 °C in: a) CH_4 (dashed) and H_2 (solid), b) CH_4/H_2S (5000 ppm, dashed) and H_2/H_2S (5000 ppm, solid), for an anode impregnated six times.

was always observed with pure methane and, to date, only assumptions could be made about this phenomenon as it was not the purpose of this work. Our previous work [15] performed on sour gas may be a basis for an explanation of these observed I/V curve shapes. However, as a regular cell is supposed to be efficient at high voltage, we chose to consider the maximum power density. In addition, it should be mentioned that carbon deposition occurs while running under pure methane.

Fig. 6a (solid) was obtained using pure H_2 as feed. The maximum current density and the maximum power density were lower than those previously reported [15,20]. At potentials less than 0.5 V there was a small mass transfer blocking effect. This effect is unusual as the oxidation process for H_2 is not considered to be complex. The mass transfer blocking effect appears to arise from a smaller amount of impregnated LSBT compared with conventional powder mixtures.

Fig. 6b (dashed) shows the performance using sour gas. As expected, the presence of H_2S in CH_4 improved the performance dramatically, and provided the typical I/V curve shape obtained using sour gas as feed [15]. In this specific case the performance of the cell was more strongly enhanced by the presence of H_2S when compared with previous data [15,20], while the I/V curve shape was similar to those previously reported [15]. The maximum power density was 75 mW cm^{-2} (uncompensated) and the maximum current density was 153 mA cm^{-2}. Unlike pure methane, tests performed under sour gas do not promote carbon deposition.

Fig. 6b (solid) was obtained using H_2/H_2S as feed. As reported elsewhere [15] the improvement in performance compared to the use of pure H_2 was dramatic, to a maximum power density of 137 mW cm^{-2} (uncompensated) and maximum current density of 600 mA cm^{-2}. There was no apparent mass transfer blocking effect, and the I/V curve had the expected shape.

In general, when compared with the use of conventional powder mixtures (50/50 wt% LSBT/YSZ), the use of porous YSZ impregnated with LSBT did not make a significant change to the overall I/V curve behavior. However, there were distinct differences: the performances when using pure H_2 or H_2/H_2S were lower than those for mechanically mixed anode material, while the performances using either CH_4 or CH_4/H_2S were higher for the impregnated anodes. Based on these observations, it appears that LSBT impregnated in small quantities promotes the surface oxidation process for CH_4, but is detrimental to the oxidation process for H_2 occurring deeper within the anode. Regarding the low power densities, recall that the tested cells use a thick electrolyte and as such cannot be compared with a commercially viable system.

3.2.3. Comparison tests

Button cells were tested to evaluate the impact of the level of impregnation on the overall performance of LSBT/YSZ. Fig. 7 compares the performance with the number of times LSBT was impregnated into porous YSZ. The temperature for each test was 850 °C and the sequence used was: H_2, H_2/0.5%H_2S, CH_4/0.5% H_2S (sour gas) and CH_4. As the cell is electrolyte supported and as the fuel contains 5000 ppm H_2S, comparison with other SOFC systems must be done with caution.

Pure H_2 provided maximum power density of 20 mW cm^{-2} for the anode having six impregnations. Thereafter, varying the number of impregnations did not significantly change the maximum power density. For the case of pure H_2, impregnation is not a good method as the amount of LSBT remains low, which may indicate that the hydrogen oxidation proceeds in bulk and is not only a surface phenomenon.

CH_4 provided a maximum power density of 24 mW cm^{-2} for the anode having eight impregnations; as for H_2, the 10th impregnation slightly decreased the performances. Compared with poisoned gases, methane exhibits similar behavior as hydrogen but unlike the latter, the produced power in CH_4 is seriously activated by the presence of LSBT as the performances are multiplied by 10 between pure YSZ and YSZ impregnated at 18% LSBT.

When the feed was CH_4/0.5% H_2S (sour gas) the power density consistently was higher than in pure H_2, from double for low amounts of LSBT to four times higher for the anode with six impregnations. While six impregnations provided maximum power density of 84 mW cm^{-2} further increasing the number of

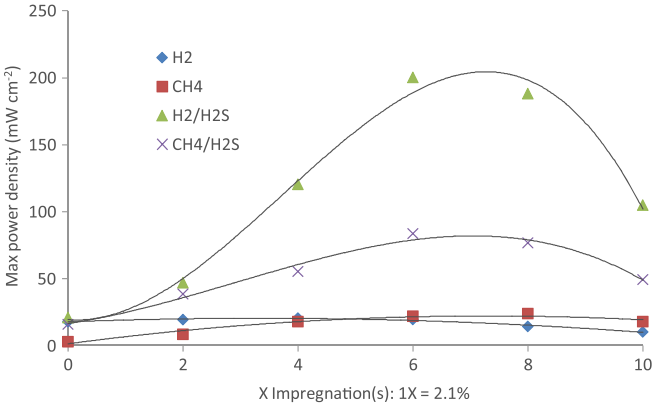

Fig. 7. Dependence of compensated maximum power density at 850 °C on the number of times LSBT was impregnated into YSZ.

impregnations led to dramatically decreased performance. This trend was also indicated weakly when using pure H_2.

Finally, H_2/0.5%H_2S used as fuel provided the best performance, achieving 200 mW cm^{-2} for the anode with six LSBT impregnations. Again, the performance decreased as the number of impregnations was increased above six.

4. Conclusions

New anode materials were prepared comprising YSZ impregnated with different amounts of $La_{0.4}Sr_{0.5}Ba_{0.1}TiO_3$ (LSBT) as both catalyst and electronic conductor. YSZ matrix microstructures produced using two different pore formers were compared, and PMMA was found to provide a superior, isotropic pore structure which was readily impregnable, in contrast to graphite. The catalytic activity of the anodes so formed increased with the amount of LSBT up to about 12.6%, but any further increase in LSBT diminished performance due to hindrance of access to active sites. Comparing performances of impregnated anodes with those prepared by mechanical mixing, impregnation gave poorer performance for conversion of H_2 as fuel and improved that for conversion of CH_4. When 5000 ppm H_2S was present in the feed, the performance for conversion of both H_2 and CH_4 was improved. Impregnation appears to be a better choice for anode preparation than powder mixtures, as only one-fourth the amount of catalyst is required to obtain similar performance. Moreover, the impregnation process allows construction of anode supported SOFC membranes.

Acknowledgments

This research was supported through funding to the NSERC Solid Oxide Fuel Cell Canada Strategic Research Network from the Natural Science and Engineering Research Council (NSERC) and other sponsors listed at http://www.sofccanada.com/.

References

[1] M. Gong, X. Liu, J. Trembly, C. Johnson, Journal of Power Sources 168 (2007) 289.
[2] M. Alifanti, R. Auer, J. Kirchnerova, F. Thyrion, P. Grange, B. Delmon, Applied Catalysis B: Environmental 41 (2003) 71.
[3] K. Haga, S. Adachi, Y. Shiratori, K. Itoh, K. Sasaki, Solid State Ionics 179 (2008) 1427.
[4] J.P. Trembly, A.I. Marquez, T.R. Ohrn, D.J. Bayless, Journal of Power Sources 158 (2006) 263.
[5] Y. Matsuzaki, I. Yasuda, Solid State Ionics 132 (2000) 261.
[6] A.A. Davydov, V.I. Marshneva, M.L. Shepotko, Applied Catalysis A: General 244 (2003) 93.
[7] K.T. Chuang, J.-L. Luo, A.R. Sanger, Chemical Industry and Chemical Engineering Quarterly/CICEQ 14 (2008) 69.
[8] J.F.B. Rasmussen, A. Hagen, Journal of Power Sources 191 (2009) 534.
[9] D.P. Fagg, V.V. Kharton, A.V. Kovalevsky, A.P. Viskup, E.N. Naumovich, J.R. Frade, Journal of the European Ceramic Society 21 (2001) 1831.
[10] X. Sun, S. Wang, Z. Wang, X. Ye, T. Wen, F. Huang, Journal of Power Sources 183 (2008) 114.
[11] K. Ahn, S. Jung, J.M. Vohs, R.J. Gorte, Ceramics International 33 (2007) 1065.
[12] X. Huang, H. Zhao, X. Li, W. Qiu, W. Wu, Fuel Cells Bulletin 2007 (2007) 12.
[13] O.A. Marina, N.L. Canfield, J.W. Stevenson, Solid State Ionics 149 (2002) 21.
[14] R. Mukundan, E.L. Brosha, F.H. Garzon, Electrochemical and Solid-State Letters 7 (2004) A5.
[15] A.L. Vincent, J.-L. Luo, K.T. Chuang, A.R. Sanger, Applied Catalysis B: Environmental 106 (2011) 114.
[16] T.Z. Sholklapper, C.P. Jacobson, S.J. Visco, L.C. De Jonghe, Fuel Cells 8 (2008) 303.
[17] J. San Ping, Materials Science and Engineering A 418 (2006) 199.
[18] A.R. Hanifi, A. Shinbine, T.H. Etsell, P. Sarkar, International Journal of Applied Ceramic Technology (2012). doi:10.1111/j.1744-7402.2011.02617.x.
[19] A.R. Hanifi, A. Torabi, T.H. Etsell, L. Yamarte, P. Sarkar, Solid State Ionics 192 (2011) 368.
[20] A. Vincent, J.-L. Luo, K.T. Chuang, A.R. Sanger, Journal of Power Sources 195 (2010) 769.